

Domain Structure of Self-Assembled Dodecanethiol Monolayers on Gold

C. Schönenberger, J. Jorritsma, J. A. M. Sondag-Huethorst, and L. G. J. Fokkink

*Philips Research Laboratories
P.O. Box 80.000
5600 JA Eindhoven
The Netherlands.*

Abstract. The positional order of dodecanethiol monolayers self-assembled on Au(111) is investigated with scanning-tunneling microscopy using ultra-high tunneling resistances $R_t \geq 300 \text{ G}\Omega$. We have studied two kinds of monolayers prepared (a) by immersion of the Au substrate into a methanoic thiol solution (as-adsorbed films), and (b) by an additional ex-situ heat treatment (annealed films). The head-group of the molecules are found to chemisorb in the commensurate $\sqrt{3} \times \sqrt{3}$ overlayer of the Au(111) surface. As-adsorbed monolayers can be characterized by an assembly of nearest-neighbor (nn) rows of molecules with many missing nn-rows. Annealed films, on the other hand, are characterized by a 2×4 superstructure and zig-zag shaped rows of missing chemisorbed molecules. The two distinct structures are proposed to originate from two different lattices of the carbon-backbone orientational degree of freedom. Annealed films show, in addition, a considerable reduction of defect structures.

1. Introduction

Self-assembled monolayers (SAMs) are crystalline chemisorbed organic monolayers (MLs) formed on a solid substrate by the spontaneous organization of molecules [1]. The possibility to functionalize the molecules enables the engineering of surfaces providing model-systems for the investigation of transport processes through membranes and for studies on wetting, adhesion and passivation [2-3]. Among the various molecule-substrate pairs, *n*-alkanethiols ($SH-(CH_2)_{n-1}-CH_3$) adsorbed onto Au are a popular combination, since the films are easy to prepare and believed to be dense and of high structural quality [3-7].

The self-assembly process of alkanethiols on Au is initiated by strong chemical interactions between the sulfur head-group and the Au surface which is believed to result in chemisorption of the molecules as thiolates, forcing them to adsorb commensurate with the Au lattice [6-13]. A crystalline film at room temperature can only be formed if the attractive tail-tail interaction due to lateral van der Waals forces is strong enough to align the tails in parallel [3,5]. This is the case for sufficiently long chains, $n \gtrsim 10$.

Using a variety of techniques such as helium scattering, electron and X-ray diffraction the sulfur head-groups of the molecules were found to bind to the Au(111) surface in the commensurate $\sqrt{3} \times \sqrt{3} R30^\circ$ overlayer structure [3,5-7,9-13]. In addition, numerical modelling [14-15], as well as IR spectroscopy [5,16-17] and X-ray diffraction [10,13,18] suggest that the tails of the molecules are tilted by $\approx 30^\circ$ away from the surface normal.

In this paper we briefly review our results obtained on dodecanethiol ($n = 12$) monolayers on Au(111), emphasizing our view on the difference in the domain structure of as-adsorbed and annealed films. A more detailed account of this work will be published elsewhere [18]. Recently, we have demonstrated that atomic resolution can reliably be obtained if large tunneling resistances $R_t \gtrsim 100 \text{ G}\Omega$ are used [19]. Previous STM studies of similar films, obtained using lower tunneling resistances, had in common the observation of unexpected and striking depressions appearing as 'holes' in STM

micrographs [20-22]. Possible models for these depressions included holes or region of disorder in the monolayers. We have demonstrated that the molecular structure within depressions is indistinguishable from the the rest of the surface which has allowed us to reject the two models above [19]. Our result lend strong support to the the model first suggested by Edinger et al. [22]: the apparent 'holes' in STM micrographs are depressions in the Au surface originating from an etching process during the adsorption and organization process of the molecules. In the mean time this etching model has received further support [23-24].

2. Experimental

Our monolayers are prepared on (111)-oriented Au films (grown epitaxially on mica) by immersion in a dodecanethiol solution (3.5 mM in methanol) held at a controlled temperature of (21 °C) during a duration t_i ranging from hours to days [24]. Prior to immersion the Au substrates are first cleaned in a UV-ozone reactor for 15 minutes. After the immersion the films are carefully rinsed to remove all weakly adsorbed species, dried, and then imaged by STM within one day. Such films will be termed *as-adsorbed films* in the following. Measured contact angles [24] for C_{12} monolayers as a function of immersion time t_i agree with results from the literature [3].

Annealed dodecanethiol monolayers, termed *annealed films* in the following, were first prepared as described above. Then, they were placed onto a Cu-block which was located in an oven at a temperature $T_a = 60 - 120$ °C for a duration t_a ranging from 1 minute to 1 hour. The temperature was regulated and measured directly on the Cu-block using a thermocouple. After annealing, the samples were rapidly quenched to room temperature (RT) by placing them onto a second large Cu block kept at RT. With this procedure we attempted to freeze in the structure present at the annealing temperature. That this was indeed the case was verified by heating up two samples directly on the STM while simultaneously measuring images (in-situ heating).

The organic films were found to be stable for at least one week as evidenced by the absence of structural changes within this period upon re-imaging. All micrographs have been obtained in the constant tunneling current mode at scan-rates of $\approx 0.1 - 1$ $\mu\text{m/s}$. The greyscale images represent the apparent surface topography in a conventional manner: white areas are topographically higher than black ones. We have used mechanically cut Pt/Rd wires as tips and, in general, imaged each sample with several different tips in order to distinguish real surface structures from tip-induced artefacts. Ultra-low tunneling currents I_t ($I_t = 1 - 10$ pA) were used to image the monolayers. In most cases the tip voltage U_t with respect to the sample was negative in the range of 10 mV to 1 V. The molecular structures, however, were found to be independent of the bias polarity. In the following we will always refer to the tip-voltage U_t with respect to the Au substrate.

3. Image Contrast for Dodecanethiol Monolayers

Nondestructive imaging with atomic-scale resolution is possible for alkanethiols with chains that are not too long, $n \lesssim 14$. In order to understand that a large tunneling resistance (which in STM corresponds to a larger tip-substrate separation) and shorter chain molecules are needed, we mention that the alkane tails of the thiol molecules are extremely good insulators (electronic band-gap ≈ 9 eV). The electrical tunnel current necessary for STM operation therefore flows from the tip to the conducting Au-substrate either directly or via a possible interface state located at the sulfur. Hence, we expect to either image the Au surface or the sulfur overlayer due to the adsorbed thiol molecules (the alkane tails of the molecules cannot be imaged). Since the typical tip-substrate distance in STM is of the order 10 Å, the tip may penetrate the molecular layer for long tail molecules or low tunneling resistances. The resulting interaction forces can become so strong that scanning the tip may destroy the assembly. We demonstrate next that a high tunneling resistance is a prerequisite for imaging the molecular monolayer. In contrast, at low tunneling resistances, the Au substrate is imaged instead of the thiol monolayer.

Fig. 1 shows two typical STM micrographs of the same surface area of an as-adsorbed dodecanethiol monolayer obtained for two different tunneling resistances R_t . Fig. 1a was obtained at $R_t = 25 \text{ G}\Omega$ and Fig. 1b at $R_t = 660 \text{ G}\Omega$. Surprisingly, there is a strong difference in image contrast depending on the magnitude of R_t . The low R_t image (Fig. 1 a) is very similar to a bare (i.e. not immersed) Au surface: flat terraces can be seen which are separated by a monoatomic Au step of height 2.4 \AA . In contrast to bare Au surfaces, however, the image reveals in addition many depressions that appear dark, i.e. topographically lowered. These depressions are the 'holes' which were found as a remarkable microscopic feature in previous STM studies of alkanethiol monolayers [20-23]. We mention that Fig. 1 a (except for some finer details) is typical for STM images obtained in previous studies.

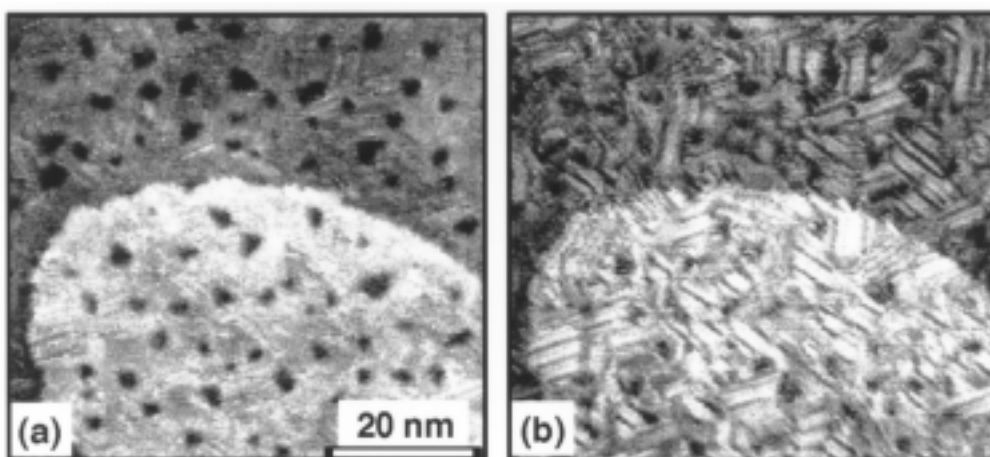


Figure 1. Demonstration of the STM contrast dependence on R_t for an *as-adsorbed* dodecanethiol monolayer on gold (immersion time 1 h). While the main features in the high $R_t = 660 \text{ G}\Omega$ image (right) are molecular domain structures, they are the holes for the low $R_t = 25 \text{ G}\Omega$ image (left).

Compared to the low R_t image (Fig. 1 a) the micrograph obtained at high R_t (Fig. 1 b) shows a lot of additional structure not (or only faintly) visible at low R_t . For example, there are pronounced dark lines which separate regions appearing bright (i.e. topographically raised). These are defect structures in the self-assembled layer which will be discussed below. By zooming on to a bright appearing region we always reliably resolve ordered periodic structures on the atomic scale with a relative large corrugation of $\approx 0.1 \text{ nm}$ provided the tunneling resistance is sufficiently large, i.e. $R_t \gtrsim 300 \text{ G}\Omega$ [18-19].

We would like to emphasize, that the corrugation of the atomic structure diminishes on lowering the tunneling resistance R_t . The molecular domain structure is only visible if R_t is sufficiently large. Moreover, imaging the surface for $R_t \lesssim 100 \text{ G}\Omega$ is found to change the atomic order inevitably or even results in the erosions of the structure [18-19]. For these lower tunneling resistances the tip obviously starts to penetrate the dodecanethiol monolayer resulting in mechanical interactions that are destructive. Non-destructive imaging of adsorbed dodecanethiols is, therefore, only possible for exceptionally large tunneling resistances which were not employed in previous STM studies.

4. Structure of the Monolayers

In this section we discuss the domain structure of dodecanethiol monolayers (MLs) as observed by STM. In discussing the structural order of self-assembled monolayers one has to distinguish positional from orientational order. The positional degree of freedom is fixed by the sulfur head groups chemisorbing at particular positions on the Au surface. The orientational order is the result of the

relative orientations of the alkane tails. More precisely, assuming the alkane tails to be rigid rods in the all-trans conformation, it has two degrees of freedom: the orientation of the carbon backbone with respect to the Au(111) lattice and its tilt with respect to the surface normal. A perfect single-crystalline monolayer is a defect free lattice of molecules with positional as well as orientational order.

Fig. 2 shows an atomically resolved STM micrograph of a dodecanethiol monolayer immersed in solution during $t_i = 17\text{h}$. This image covers a $60 \times 60\text{ nm}$ area and was obtained using $R_t = 670\text{ G}\Omega$ with a tip voltage of $U_t = -1\text{ V}$. Except for the many defect structures visible, the lattice is locally hexagonal with a nearest neighbor distance $d_{nn} \cong 5\text{ \AA}$ consistent with the $\sqrt{3} \times \sqrt{3} R30^\circ$ Au(111) overlayer structure. The three white arrows at the bottom left of Fig. 2 indicate the directions of nearest neighbors (nn) of the adatom lattice formed by the sulfur head-groups. From Helium diffraction studies [25], which probes the ordering of the alkyl endgroups (the ones forming the actual surface), it is known that the end groups are disordered at room temperature (RT), and the $\sqrt{3} \times \sqrt{3}$ ordering is only confirmed at lower temperatures. X-ray and electron diffraction techniques [9,13,16,25-26], which are more sensitive to the molecular head groups, i.e. the sulfurs, show that these are ordered at RT in the commensurate $\sqrt{3} \times \sqrt{3} R30^\circ$ Au-overlayer structure. Since we observe the $\sqrt{3} \times \sqrt{3}$ lattice for high tunneling resistances at RT, this demonstrates that the sulfur adatoms are imaged as anticipated in section 3. This implies that only information on the positional degree of order can be obtained directly. Even though STM is foremost sensitive to the head-group substrate bond, we may expect that the variation in the packing of the alkane tails arrangements affects the local-density of states probed at the Au-S bond. It could even result in a relaxation of the structure of the Au(111) surface. Hence, imaging the sulfur overlayer may indirectly give information on the unit cell of the whole molecular monolayer.

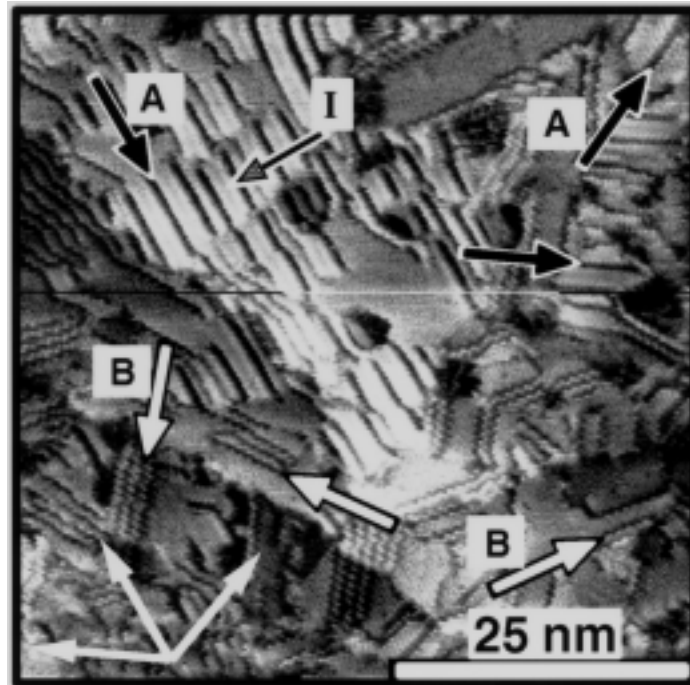


Figure 2. High-resolution atomic-scale STM image obtained at $R_t = 670\text{ G}\Omega$ ($I_t = -1.5\text{ pA}$, $U_t = -1\text{ V}$) for an *as-adsorbed* dodecanethiol monolayer (immersion time $t_i = 17\text{h}$). Apart from the locally hexagonal structure there are many visible dark-appearing line defects interpreted as originating from missing chemisorbed molecules. The straight A-defect (black arrows) is aligned along the nearest-neighbor direction of molecules and the zig-zag appearing B-defect (white arrows) along next-nearest neighbors (see model in Fig. 7).

In Fig. 2 there are two types of pronounced line defects visible, which are denoted by A and B, respectively. The A defects are dark straight lines oriented along the nn-direction (black arrows in Fig. 2), while the B line defects (white arrows in Fig. 2) appear rugged and are oriented in the direction of next-nearest neighbors (nnn) of molecules. In terms of the underlying Au(111) lattice the nn-direction of molecules is indexed as $[1\bar{2}1]$ and the nnn-direction as $[1\bar{1}0]$. These line defects appear topographically lower (dark) by as much as $\delta s \approx 3 \text{ \AA}$ and no structure can be resolved within the lines. Since the apparent depth roughly corresponds to the difference in measured height between a bare Au surface and chemisorbed thiol molecules (not shown, see Ref. 18), these defects are interpreted as rows of missing molecules. A model of the two types of missing rows is presented in Fig. 3. The A-type missing row results from removing a straight line of nn-molecules. The B-type missing row is the result of removing pairs of molecules resulting in a zig-zag pattern. In Fig. 3, one A (missing -) row and two B rows (missing zig-zag rows) are shown. In the model of Fig. 3 we assume that all molecules adopt one and the same adsorption site of three possibilities given by the unit cell of the $\sqrt{3} \times \sqrt{3}$ structure. However, we have found evidence for the presence of phase-shift domain boundaries [18]. Thermal drift and nonlinearities in the scanner of the microscope render the estimation of the density of phase-shift domain boundaries difficult. In a recent X-ray diffraction study of similar films the correlation length for the positional order was measured to be only $\approx 10 \text{ nm}$ [13]. In view of this short correlation length we cannot exclude the possibility that visible defects in Fig. 2 involve phase shifts as well.

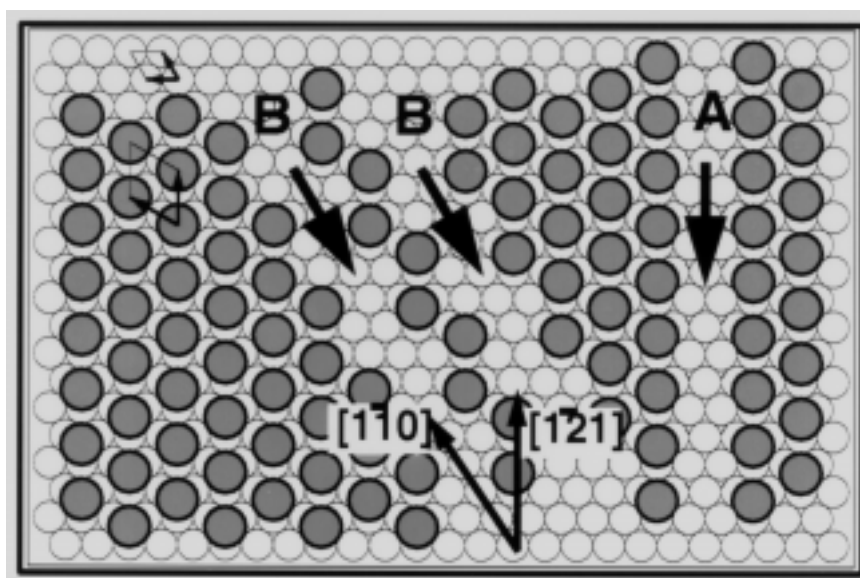


Figure 3. Proposed model for the two types of line defects visible in STM micrographs of thiol monolayers. In the A-defect a row of nearest-neighbor (chemisorbed) molecules is missing. In the B-defect a 'zig-zag' row oriented along the next-nearest neighbors is missing. Small circles represent Au surface atoms and the larger dark shaded ones chemisorbed sulfur head-groups of thiol molecules.

In Fig. 2 one can clearly see that many of the A-type missing rows do not appear randomly on the surface. Often, there are missing A-type rows that separate islands of equal width. Such an island is marked by an arrow denoted by I in Fig. 2. We observe such islands in three possible orientations, which reflects the three-fold symmetry of the underlying Au(111) lattice. A Fourier transformation of images as in Fig. 2 shows peaks at a smaller spatial frequency than the frequency which corresponds to the nearest neighbor sulfur adlattice. From the statistical analysis of several images we conclude

that these islands most likely contain four nn-rows of molecules. There is almost never a single row found. Pairs of nn-rows, however, are also common (see in Fig. 2 to the left of arrow I).

In addition, to the structure based on a periodic packing of nearest-neighbour rows, a superstructure oriented along the nnn-row direction is observed on some areas of *as-adsorbed* films, in particular on those films, which were immersed during a longer period of time ($t_i > 10$ h). An image of such a reconstructed area is shown in Fig. 4a. A weak modulation of ≈ 0.5 Å of the corrugation is superimposed on the conventional $\sqrt{3} \times \sqrt{3}$ pattern. The superstructure results in alternating lines of depressions oriented along the next-nearest neighbor (nnn) direction of molecules. Close inspection of STM images shows that the apparent corrugation is due to a zig-zag pattern of molecules. This is schematically shown in Fig. 4b. The darker shaded circles correspond to sulfur atoms that appear topographically lower while the brighter circle represents apparently raised sulfur atoms. This pattern has a 2x4 periodicity with respect to the $\sqrt{3} \times \sqrt{3}$ overlayer lattice.

We propose that this structure is identical to the 2x4 structure found recently by Camillone et al. for n-octadecanethiol ML on Au(111) using He-diffraction techniques [11]. Similar superlattice diffraction peaks were observed in the grazing incidence X-ray diffraction study by Fenter et al. for alkanethiols of different chain length [13] and, very recently, in STM studies [27]. The proposed model for this superstructure consists of molecules that alternate their carbon backbone orientation.

Finally, we would like to point out that the B-type missing rows shown in Fig. 2,3 are made up of the same pattern that results in the 2x4-superlattice structure. The B-type missing row is just formed by removing one zig-zag row of molecules in Fig. 4b. It is therefore tempting to assume that B-type missing row defects are related to the 2x4 superstructure.

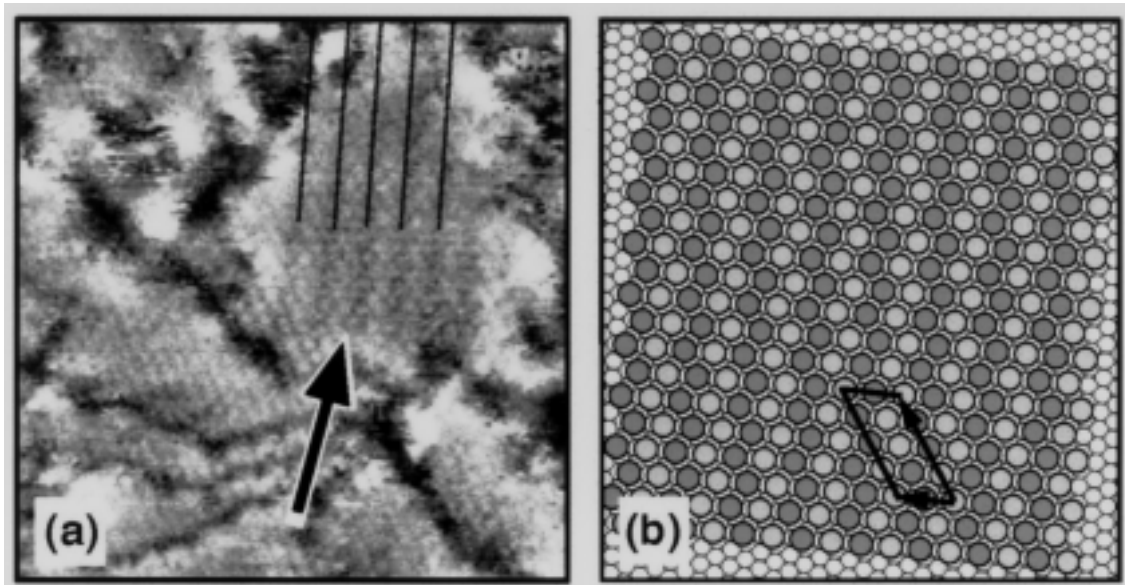


Figure 4. Left: STM micrograph of size 17×17 nm² obtained with $R_t = 500$ GΩ on an *as-adsorbed* dodecanethiol film immersed during 2 days. The arrow points to an ordered island on which a superstructure is visible. Right: Schematics of the apparent corrugation of the superstructure due to the zig-zag formation of molecules. The lighter (darker) shaded circles represent apparently raised (suppressed) sulfur adatoms. The 2x4 unit cell of the superstructure is indicated in (b).

5. Annealed- vs. as-Adsorbed monolayers

The study of *annealed* alkanethiol monolayers was initiated by the work of Fenter et al. [13]. Their grazing-incidence x-ray diffraction study of thiol monolayers on Au revealed a striking increase of the domain size (estimated from the diffraction linewidth) upon annealing the monolayers. Whereas *as-adsorbed* monolayers (MLs) were found to have a domain size of ≈ 10 nm only, this size increases to ≥ 100 nm for films *annealed* at 90°C .

In Fig. 5 we present a comparison of two images representative for *as-adsorbed* (Fig. 5a) and *annealed* (Fig. 5b) dodecanethiol monolayers. The *as-adsorbed* monolayer was obtained by immersion during 4 hours and the image in Fig. 5a represents a 70×70 nm² area. The *annealed* film was obtained by annealing at $T_a \approx 85^\circ\text{C}$ during $t_a = 20$ min and the image in Fig. 5b represents an area of 150×150 nm². The inset in Fig. 5b shows a smaller area with atomic-scale resolution. In the inset the $\sqrt{3} \times \sqrt{3}$ structure of the thiol ML is visible also within a hole (see black arrow). This demonstrates that these 'holes' are covered with thiol molecules and similarly ordered as on terraces [19].

For *as-adsorbed* monolayers, the characteristic islands (marked by arrows denoted I), consisting of four rows of nn-molecules, together with missing A-type rows (missing nn-rows) are seen in Fig. 5a to be the predominant feature. In case of *annealed* films, most line defects (see e.g. black arrow in Fig. 5b) are oriented along the nnn-directions and are therefore interpreted to be B-type defects (missing zig-zag rows). In contrast, *as-adsorbed* films contain much more A-type missing rows (missing rows of nn-molecules). In addition to the missing zig-zag rows, the 2×4 -superstructure is observable over large parts of surface for *annealed* films (not shown).

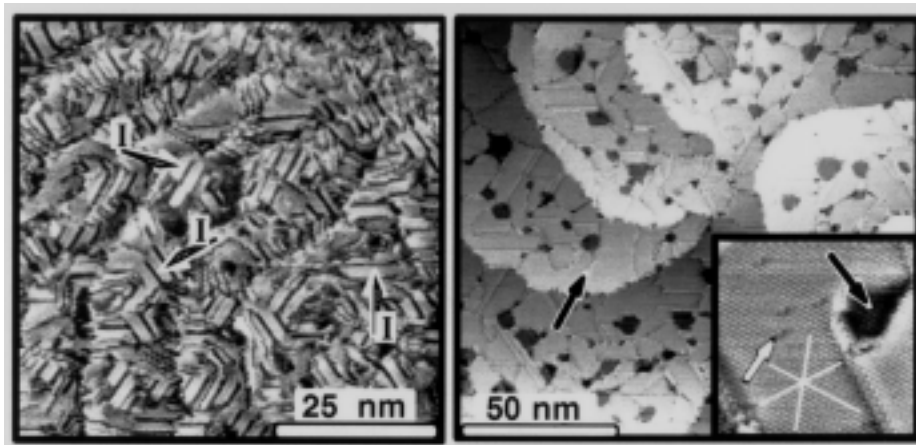


Figure 5. a: STM micrograph obtained at $R_t = 670$ G Ω representative for *as-adsorbed* dodecanethiol films (immersion time 4 h). The majority of atomic-scale line defects are A-type straight line defects, i.e. missing rows of nearest neighbor (nn) chemisorbed molecules. These defect lines preferentially separate islands of four nn-rows, see for example arrow I (also in Fig. 2). b: Large scale (150×150 nm²) STM image ($R_t = 670$ G Ω) of a dodecanethiol monolayer *annealed* at $T_a \approx 85^\circ\text{C}$ during 20 min. The majority of visible line defects are missing zig-zag rows. Inset: High resolution zoomed-in micrograph of size 17×17 nm². The hexagonal structure, also clearly visible in the hole (black arrow), contains a few point defects (white arrow). The three white lines indicate nearest neighbor directions.

The average size of an area in Fig. 5b bounded by line defects is ≈ 15 nm. This is at least a factor 2 – 3 larger than what is observed for the *as-adsorbed* films. Even though it is tempting to assign this number to the actual domain size, one has to be careful in doing this. We recall that STM images the sulfur head group and therefore only positional order is directly accessible. Since A- and B-type defects without phase shifts do not reduce the coherence length of the positional degree of freedom,

we expect the domain size to be larger than the size of the areas bounded by the visible line defects. In the X-ray diffraction study of Fenter et al. [13] the domain size of identically prepared *annealed* films was found to be ≥ 100 nm, i.e. much larger than the 15 nm sized areas in Fig. 5b. The missing zig-zag rows do therefore not mark domain boundaries of the positional degree of freedom. Most likely, the entire area in Fig. 5b is perfectly positionally ordered, i.e. all sulfur head-groups are chemisorbed in a $\sqrt{3}x\sqrt{3}$ lattice without phase shift domain boundaries. We can think of two possible origins for the presence of the still many missing zig-zag rows for *annealed* films. These defect rows are either formed by a strained monolayer and needed to relax the strain, or, they mark domain boundaries of the orientational degree of freedom, i.e. different tilt orientation of the molecules. At present we can not distinguish between these two possibilities. He-diffraction experiments on *post-annealed* films would help to resolve this issue.

6. Discussion

In this section we briefly discuss the major structural differences between *as-adsorbed* and *annealed* films in context with a molecular dynamics (MD-) simulation recently performed by Mar and Klein [15]. In this calculation different possible chain packings with two and four thiol molecules per unit cell were compared. The results show that the 2x1 'herringbone' structure is energetically more favourable than the 2x4 superstructure by ≈ 0.9 kcal/mol. These two structures are schematically shown in Fig. 6. The large circles represent sulfur head-groups on the Au(111) surface. The difference in shading is due to two different carbon backbone orientations of the alkane tails marked by arrows in Fig. 6. Fig. 6a shows the 2x1 'herringbone' structure which represents the most efficient packing for 2 chains per unit cell. The 2x4 structure shown in Fig. 6b represents one possibility of several calculated 2x4 structures that slightly differ in the carbon backbone orientation. The two structures in Fig. 6 can be described by alternating rows of molecules with two different backbone orientations. In the 2x1 structure nn-rows alternate and in the 2x4 structure zig-zag rows oriented along the nnn-direction.

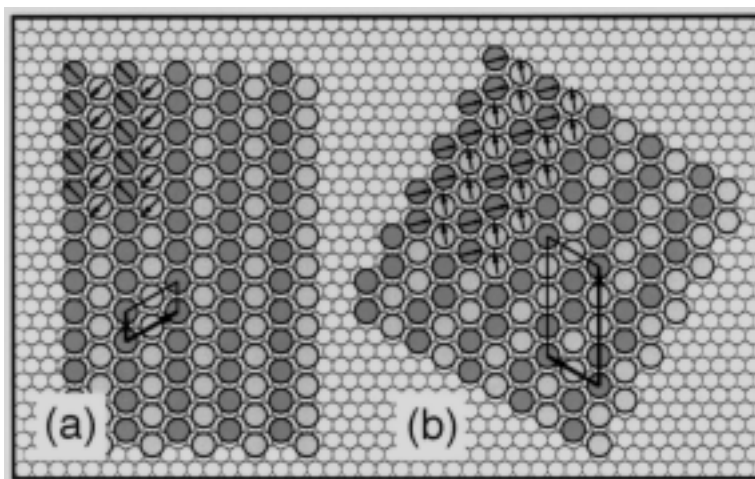


Figure 6. Two possible and distinct domain structures (discussed in Ref. 15) that may explain the affinity for nearest-neighbor row structures in *as-adsorbed* films, on the one hand, and for zig-zag patterns (2x4 superstructure and missing zig-zag rows) predominately observed in *annealed* films, on the other hand. The shaded circles represent sites of adsorbed molecules with a carbon-backbone orientation indicated by the arrows. (a) is the 2x1 herringbone structure which closely resembles the optimized alkane packing and (b) is one of the possible 2x4 structures.

Our STM study shows that *as-adsorbed* films are characterized by structures that are made up of paired nn-rows of molecules together with A-type missing rows, which are also oriented along the nn-direction. In contrast, *annealed* films have a preference for the formation of the 2x4 superstructure consisting of alternating zig-zag rows of molecules oriented along the nnn-direction together with B-type missing rows.

We propose that the nn-formation of *as-adsorbed* films corresponds to the 2x1 'herringbone' structure in Fig. 6a and the zig-zag structure of *annealed* films corresponds to the 2x4 structure shown in Fig. 6b. Since the 2x4 structure is characteristic for *annealed* films, the experiment then suggests that this structure is energetically more favourable than the 2x1 structure. That this is in contrast to the MD-simulation may be the result of the omission of structural relaxations of the Au(111) surface in the numerical calculation.

7. Summary

Using ultrahigh tunneling resistances $R_t \gtrsim 300 \text{ G}\Omega$ we have succeeded in imaging (at room temperature) self-assembled monolayers of n-alkanethiol molecules $\text{SH}-(\text{CH}_2)_{n-1}-\text{CH}_3$ ($n = 10, 12$) on Au(111) with atomic scale resolution [19]. The basic structure is a lattice with a three times larger unit cell relative to the Au(111) surface consistent with the $\sqrt{3}x\sqrt{3}$ overlayer found by other structure analysis techniques [3,5-7,9-13]. Since the alkane tail termini of the molecules are disordered at room temperatures [25], we conclude that STM is exclusively sensitive to the sulfur head groups. Only information on the positional order of the molecules can therefore be obtained directly.

STM enables the characterization of atomic-scale defect structures. Most prominent are line defects interpreted as rows of missing chemisorbed molecules. There are two kinds of such defects: a straight one oriented along the nearest-neighbor (nn) adlattice direction (missing nn-rows) and a zig-zag shaped missing row defect oriented along the next nearest-neighbor direction (missing zig-zag row). In order to avoid a misunderstanding we would like to emphasize that with missing molecule an adsorption site is meant where apparently no *chemisorbed* molecule is present. The presence of physisorbed molecules on these sites cannot be excluded.

Our analysis focusses on dodecanethiol ($n = 12$) monolayers either prepared by immersion for a few hours into a 3.5 mM concentrated thiol solution in methanol – *as-adsorbed* films, or prepared by additionally annealing the films at $T_a \approx 90 \text{ }^\circ\text{C}$ ex-situ – *annealed* films (the results for other annealing temperatures are discussed in Ref. 18). The characteristic structures for the films prepared by these two methods are different. *As-adsorbed* films are characterized by many missing nn-rows which are alternating regularly with four rows of chemisorbed molecules. On *annealed* monolayers we find far less line defects, which are now of the missing zig-zag type. In addition, on a large fraction of the surface a longer wavelength modulation is superimposed on the $\sqrt{3}x\sqrt{3}$ pattern. This results in a superstructure with 2x4 periodicity. Interestingly, this 2x4 superstructure is made up of pairs of zig-zag rows and it is therefore likely that the missing zig-zag rows are related to this 2x4 structure.

The two different characteristics for *as-adsorbed* and *annealed* monolayers are proposed to originate from two distinct ordered structures of the molecular assembly including in addition to the positional order the carbon-backbone orientational degree of freedom.

Acknowledgements

We are grateful to G. H. L. Brocks, H. B. Elswijk, and N. Kramer for stimulating discussions and useful suggestions, and to H. C. Donkersloot, M. T. Johnson, and J. M. Kerkhof for the growth of the Au substrates. One of us (C. S.) would like to thank H. van Houten for continuous support and valuable suggestions.

References

- [1] For a review see: a) A. Ulman *An Introduction to Ultrathin Organic Films from Langmuir-Blodgett to Self-Assembly*, (Academic, Boston 1991). b) G. M. Whitesides and P. E. Laibinis, *Langmuir* (1990), 6, 87.
- [2] R. G. Nuzzo and D. L. Allara *J. Am. Chem. Soc.* (1983), 105, 4481. C. D. Bain and G. Whitesides, *Science* (1988) 240, 62. C. D. Bain, J. Evall, and G. Whitesides, *J. Am. Chem. Soc.* (1989), 111, 7155. J.-E. Sundgren, P. Bodö, B. Ivarsson, and I. Lundström, *J. Colloid Interface Sci.* (1986), 113, 43. L. Bertilsson and B. Liedberg, *Langmuir* (1993), 9, 141. J. J. Hickman, D. Ofer, C. Zou, M. S. Wrighton, P. E. Laibinis, and G. M. Whitesides, *J. Am. Chem. Soc.* (1991), 113, 1128. J. A. M. Sondag-Huethorst, L. G. J. Fokkink, *J. Electroanal. Chem.* (1994), 367, 49.
- [3] C. D. Bain, E. B. Troughton, Y.-T. Tao, J. Evall, G. Whitesides, and R. G. Nuzzo, *J. Am. Chem. Soc.* (1989), 111, 321.
- [4] T. T. T. Li and M. J. Weaver, *J. Am. Chem. Soc.* (1984), 106, 6107.
- [5] M. D. Porter, T. B. Bright, D. L. Allara, and C. E. D. Chidsey, *J. Am. Chem. Soc.* (1987), 109, 3559.
- [6] R. G. Nuzzo, B. R. Zegarski, and L. H. Dubois, *J. Am. Chem. Soc.* (1987), 109, 733.
- [7] C. E. D. Chidsey and D. N. Loiacono, *Langmuir* (1990), 6, 682.
- [8] R. G. Nuzzo, B. R. Zegarski, and L. H. Dubois, *J. Am. Chem. Soc.* (1987), 109, 733. D. E. Weisshaar, B. D. Lamp, and M. D. Porter, *J. Am. Chem. Soc.* (1992), 114, 5860. B. Hagenhoff, A. Benninghoven, J. Spinke, M. Liley, and W. Knoll, *Langmuir* (1993), 9, 1622.
- [9] L. Strong and G. M. Whitesides, *Langmuir* (1988), 4, 546.
- [10] M. G. Samant, C. A. Brown, and J. G. Gordon II, *Langmuir* (1991), 7, 437.
- [11] N. Camillone III, C. E. D. Chidsey, G.-Y. Liu, and G. Scoles, *J. Chem. Phys.* (1993), 98, 3503.
- [12] N. Camillone III, C. E. D. Chidsey, P. Eisenberger, P. Fenter, J. Li, K. S. Liang, G.-Y. Liu, and G. Scoles, *J. Chem. Phys.* (1993), 99, 744.
- [13] P. Fenter, P. Eisenberger, and K. S. Liang, *Phys. Rev. Lett.* (1993), 70, 2447.
- [14] A. Ulman, J. E. Eilers, and N. Tillman, *Langmuir* (1989), 5, 1147. J. Hautman and M. L. Klein, *J. Chem. Phys.* (1989), 91, 4994. J. Hautman, J. P. Bareman, W. Mar, and M. Klein, *J. Chem. Soc. Faraday Trans.* (1991), 87, 2031.
- [15] W. Mar and M. Klein, *Langmuir* (1994), 10, 188.
- [16] R. G. Nuzzo, L. H. Dubois, and D. L. Allara, *J. Am. Chem. Soc.* (1990), 112, 558.
- [17] R. G. Nuzzo, E. M. Korenic, and L. H. Dubois, *J. Chem. Phys.* (1990), 93, 767.
- [18] C. Schönenberger, J. Jorritsma, J. A. M. Sondag-Huethorst, and L. G. J. Fokkink, submitted to *J. Phys. Chem.*

- [19] C. Schönenberger, J. A. M. Sondag-Huethorst, J. Jorritsma, and L. G. J. Fokkink, *Langmuir* (1994), 10, 611.
- [20] L. Häußling, B. Michel, H. Ringsdorf, and H. Rohrer, *Angew. Chem. Int. Ed. Engl.* (1991), 30, 569. C. A. Widrig, C. A. Alves, and M. D. Porter, *J. Am. Chem. Soc.* (1991), 113, 2805. C. A. Alves, E. L. Smith, C. A. Widrig, and M. D. Porter, *SPIE* (1992), 1636, 125. C. A. Alves, E. L. Smith, and M. D. Porter, *J. Am. Chem. Soc.* (1992), 114, 1222.
- [21] Y-T. Kim and A. J. Bard, *Langmuir* (1992), 8, 1096. Li Sun and R. M. Crooks, *J. Electrochem. Soc.* (1991), 138, L23. M. Mizutani, D. Anselmetti and B. Michel, in *Proc. NATO ASI Computations on the Nano-Scale*, P. E. Blöchl, C. Joachim, A. J. Fisher, eds., (Kluwer Academic, 1993). M. Mizutani, B. Michel, R. Schierle, H. Wolf, and H. Rohrer, *Appl. Phys. Lett.* (1993), 63, 147.
- [22] K. Edinger, A. Götzhäuser, K. Demota, Ch. Wöll, and M. Grunze, *Langmuir* (1993), 9,4.
- [23] R. L. McCarley, D. J. Dunaway, and R. J. Willicut, *Langmuir* (1993), 9, 2775. J.P. Bucher, L. Santesson, and K. Kern, *Langmuir* (1994), 10, 979.
- [24] J. A. M. Sondag-Huethorst, C. Schönenberger, and L. G. J. Fokkink, to appear in *J. Phys. Chem.*
- [25] C. E. D. Chidsey, G.-Y. Liu, P. A. Rowntree, and G. Scoles, *J. Chem. Phys.* (1989), 91, 4421. N. Camillone, C. E. D. Chidsey, G.-Y. Liu, T. M. Putvinski, and G. Scoles, *J. Chem. Phys.* (1991), 94, 8493.
- [26] L. H. Dubois, B. R. Zeggarski and R. G. Nuzzo. *J. Chem. Phys.* (1993), 98, 678.
- [27] E. Delamar, B. Michel, Ch. Gerber, D. Anselmetti, H.-J. Güntherodt, H. Wolf, and H. Ringsdorf, submitted.